Elsevier Editorial System(tm) for International Journal of Thermal Sciences
Manuscript Draft

Manuscript Number: THESCI-D-12-00199R2

Title: Heat and mass transfer in a bubble plate absorber with NH3/LiNO3 and NH3/(LiNO3+H2O) mixtures

Article Type: Research Paper

Keywords: Absorption chiller; Bubble absorber; Plate heat exchanger; Ammonia; Lithium nitrate

Corresponding Author: Dr. Mahmoud Bourouis, Ph.D.

Corresponding Author's Institution: Universitat Rovira i Virgili

First Author: Cesar Oronel, Ph.D.

Order of Authors: Cesar Oronel, Ph.D.; Carlos Amaris, Ph.D. Student; Mahmoud Bourouis, Ph.D.; Manel Vallès, Ph.D.

Abstract: An experimental study of bubble absorption in a plate heat exchanger using ammonia/lithium nitrate and ammonia/(lithium nitrate + water) mixtures has been carried at operating conditions of air-cooled absorption systems driven by low temperature heat sources. An experimental test has been layout and set-up for the absorber characterization at different operation conditions. Experiments have been performed at a nominal system pressure of 510 kPa absolute using a corrugated plate heat exchanger formed by three channels in which absorption takes place in the central one.

A sensitive study of the main operating conditions such the weak solution inlet concentration and flowrate, and cooling water inlet temperature and flowrate on the absorber efficiency parameters has been performed.

For both binary and ternary mixtures, the mass absorption flux, heat transfer coefficient, subcooling and mass transfer coefficient increase as the solution flowrate increases.

The mass absorption flux achieved with the binary mixture is enhanced as the cooling-water inlet temperature decreases. This trend is reversed for the solution-side heat transfer coefficient. This is attributed to a limiting heat transfer process in the absorber at lower cooling-water inlet temperatures.

Increasing the concentration of ammonia in the binary mixture by 3 % by weight significantly reduces the mixture's capacity to absorb ammonia.

The mass absorption flux and the solution heat transfer coefficient achieved with the ternary mixture are around 1.3-1.6 and 1.4 times higher, respectively, than those of the binary mixture under similar operating conditions. This is due mainly to the lower viscosity of the ternary mixture and the high affinity of ammonia for water.

Empirical correlations for the solution Nusselt and Sherwood numbers are proposed on the basis of the experimental data presented here for the absorption of ammonia vapor by ammonia/lithium nitrate mixture in a plate heat exchanger.

Heat and mass transfer in a bubble plate absorber with $NH_3/LiNO_3$ and $NH_3/(LiNO_3+H_2O)$ mixtures

Cesar Oronel, Carlos Amaris, Mahmoud Bourouis *, Manel Vallès

CREVER – Universitat Rovira i Virgili, Av. Països Catalans No. 26,

43007 Tarragona, Spain. *Corresponding author

ABSTRACT

An experimental study of bubble absorption in a plate heat exchanger using ammonia/lithium nitrate and ammonia/(lithium nitrate + water) mixtures has been carried at operating conditions of air-cooled absorption systems driven by low temperature heat sources. An experimental test has been layout and set-up for the absorber characterization at different operation conditions. Experiments have been performed at a nominal system pressure of 510 kPa absolute using a corrugated plate heat exchanger formed by three channels in which absorption takes place in the central one.

A sensitive study of the main operating conditions such the weak solution inlet concentration and flowrate, and cooling water inlet temperature and flowrate on the absorber efficiency parameters has been performed.

For both binary and ternary mixtures, the mass absorption flux, heat transfer coefficient, subcooling and mass transfer coefficient increase as the solution flowrate increases.

The mass absorption flux achieved with the binary mixture is enhanced as the cooling-water inlet temperature decreases. This trend is reversed for the solution-side heat transfer coefficient. This is attributed to a limiting heat transfer process in the absorber at lower cooling-water inlet temperatures. Increasing the concentration of ammonia in the binary mixture by 3 % by weight significantly reduces the mixture's capacity to absorb ammonia.

The mass absorption flux and the solution heat transfer coefficient achieved with the ternary mixture are around 1.3-1.6 and 1.4 times higher, respectively, than those of the binary mixture under similar operating conditions. This is due mainly to the lower viscosity of the ternary mixture and the high affinity of ammonia for water.

Empirical correlations for the solution Nusselt and Sherwood numbers are proposed on the basis of the experimental data presented here for the absorption of ammonia vapor by ammonia/lithium nitrate mixture in a plate heat exchanger.

Keywords: Absorption chiller; Bubble absorber; Plate heat exchanger; Ammonia; Lithium nitrate

Highlights

- We carried out an experimental characterization of the absorption process with $NH_3/LiNO_3$ and $NH_3/(LiNO_3+H_2O)$ mixtures in a plate heat exchanger (PHE).
- We analyzed the effect of the main operating conditions parameters on the absorber efficiency criteria.
- We proposed empirical correlations for Nusselt and Sherwood numbers for the absorption of NH_3 vapor by $NH_3/LiNO_3$ in a PHE.

Nomenclature

A	*Heat transfer area*
Cp	*Heat capacity*
e	*Plate thickness*
F	*NH_3 mass absorption flux per heat transfer area*
h	*Heat transfer coefficient*
Km	*Mass transfer coefficient*
k	*Thermal conductivity*
LMTD	*Logarithmic Mean Temperature Difference*
$\dot{m}$	*Mass flow rate*
Nu	*Nusselt number*
P	*Pressure*
Pr	*Prandtl number*
Q	*Thermal load*
Re	*Reynolds number*
Sh	*Sherwood number*
U	*Overall heat transfer coefficient*
V	*Volumetric flow rate*
x	*NH_3 mass fraction in solution*

Subscripts:

AB	*Absorber*
Cw	*Cooling water*
Eq	*Equilibrium*
In	*Absorber inlet*
NH_3	*Ammonia*
Out	*Absorber outlet*
S	*Solution*
Sat	*Saturation state*
Sub	*Sub-cooling*
W	*Wall*

Greek letters:

ΔT	*Temperature difference*
μ	*Dynamic viscosity*
ρ	*Density*

1. Introduction

The demand for summer air conditioning continues to grow not only in the tertiary sector but also in residential applications. The corresponding demand for electric power may cause failures in the electricity supply network, which must cover increasingly higher peak loads. Furthermore, the environmental impact of these systems in terms of climate change may be very important in the future. In this context, small capacity absorption systems are becoming increasingly attractive in applications where the input energy can be obtained from solar energy. Presently, two types of heat driven technology are widely used in residential solar-air conditioning systems: the water/lithium bromide system and the ammonia/water system. These technologies have some drawbacks caused by the working fluids used.

The water–lithium bromide working pair has problems such as corrosion and vacuum operation, but the main problem is the crystallization that occurs at high cooling water temperatures. Consequently, these types of chiller usually need wet cooling towers for re-cooling in order to dissipate the heat generated internally in the absorber and condenser, thus limiting their use in the residential sector because of the cost involved and because of the risk of legionella. Furthermore, a wet cooling tower consumes large quantities of water to replenish the water that is evaporated and released from the

cooling tower. These drawbacks severely impede the use of these chillers in the domestic sector [1].

The performance of an absorption cycle using the ammonia/water working pair is lower and additionally requires higher driven temperatures. Moreover, the ammonia/water working pair has to be rectified because the absorbent (water) is relatively volatile, which means that ammonia vapor leaving the generator usually contains a significant amount of water vapor. For this reason the ammonia/water system has to include a distillation column attached to the top of the generator. Distillation of vapor increases the complexity of the plant and the fixed costs. However, because ammonia and water are mutually soluble throughout the concentration range, this working pair does not cause crystallization and thus allows the use of dry towers. Nevertheless, on hot days, the driven temperature resulting from using a dry cooling tower becomes too high for solar driven systems.

In order to overcome the limitations of the traditional working pairs, alternative working fluids such as ammonia/lithium nitrate have been proposed in the literature [2]. The advantages of this working pair over conventional water/lithium bromide are: a) it does not cause crystallization in solar air-conditioning systems and so allows the cycle to be air-cooled; b) the absorption cycle does not operate under vacuum conditions. Compared with the ammonia/water working pair, ammonia/lithium nitrate a) does not require a rectifier at the generator outlet because the absorbent is a salt, and b) can be used at a lower temperature in the generator, according to the results of the thermodynamic simulation [3,4,5,6].

However, poor results have been obtained with prototypes of absorption refrigeration machines designed initially to operate with the ammonia/water working pair [5,7,8] but loaded with the ammonia/lithium nitrate working pair. The authors of these experimental studies agree that the main reason for the poor performance is due to the high viscosity of this mixture compared with that of ammonia/water. This high viscosity reduces the performance predicted by the thermodynamic models. This reduction is higher at low cooling water temperatures because the viscosity increases drastically in the absorber.

To overcome this drawback Ehmke and Renz [9] and Bokelmann [10] proposed adding water to the binary mixture of ammonia/lithium nitrate to be used in absorption heat pumps. Later, Reiner and Zaltash [11] proposed using the ternary mixture for GAX systems as an alternative to the ammonia/water systems.

Ehmke [12] studied the effect of water on the solubility and viscosity of the ternary mixtures and suggested an optimal water mass fraction of between 0.20 and 0.25 in the absorbent mixture (lithium nitrate + water). The author also determined and correlated the density and vapor pressure of the solutions with a 0.25 water mass fraction of the absorbent mixture. Bokelmann [9] reported experimental research concerning the performances of an absorption heat pump. Similar data were also reported by Manago [13] in a study on new mixtures for absorption heat pumps that formed part of the Heat Pump Program of the International Energy Agency. Reiner and Zaltash [14] measured the densities and viscosities of ternary mixtures with an ammonia mass fraction of 0.04 and a water mass fraction of 0.605, this being a typical composition for GAX systems. They also measured the boiling point of this mixture at atmospheric pressure. Bothe [15] presented a comparative study of the ammonia/water system and the ammonia/(lithium nitrate + water) ternary mixture. The author reported that the ternary mixture had higher operation temperatures and important COP improvements in heat pump applications than did the binary. He also highlighted the need to make a minor rectification to increase the capacity. Moreno-Quintanar et al. [16] compared the effect of both the binary mixture ammonia/lithium nitrate and the ternary mixture ammonia/(lithium nitrate + water) on the performance of a solar powered intermittent absorption refrigeration system. The authors concluded that the ternary mixture produced a higher amount of ammonia during the generation when there were absorbent water concentrations of 20 % and 25 %. It was also found that with the ternary mixture the solar coefficients of performance were up to 24 % higher than those obtained with the binary mixture (varying from 0.066 to 0.093) and that the initial generation temperatures were up to 5.5 °C lower than those required for the ammonia/lithium nitrate mixture. No traces of water in the ammonia vapor were observed at any point during the experimental test.

Regarding the thermophysical properties of the binary and ternary mixtures, Libotean et al. [17, 18] presented experimental measurements and equations for calculating the vapor-liquid equilibrium and the transport properties of the binary mixture ammonia/lithium nitrate and the ternary mixture ammonia/(lithium nitrate + water) with absorbent water concentrations of 20, 25 and 30 %. Cuenca et al. [19] published experimental data of thermal conductivity for the binary mixture ammonia/lithium nitrate at temperatures ranging from 35 to 50 ºC and ammonia mass fraction in the range 0.30-0.50.

The recent solubility data compiled by Eysseltová and Orlova [20] also confirm that adding water improves the solubility of the solution, making the ternary mixture more suitable for high generation temperatures or low cooling temperatures.

The present study is part of an R&D project dealing with the experimental characterization of absorption and generation processes when ammonia/lithium nitrate and ammonia/(lithium nitrate + water) are used in plate heat exchangers at operating conditions of interest for absorption chillers. The results presented in this paper refer to the study carried out on the absorption process and research on ammonia vapour absorption into ammonia-lithium nitrate solution is limited to the papers cited in the manuscript when only the bubble absorption method is used. There is little information regarding the use of the ammonia/lithium nitrate mixture and the ternary mixture of ammonia/(lithium nitrate + water) in the absorption process. Infante Ferreira [21] presented the experimental results of using ammonia/lithium nitrate and ammonia/sodium thiocyanate in a vertical tubular bubble absorber. Cerezo et al. [22] developed a mathematical model to analyze the absorption process in a bubble absorber using ammonia/water, ammonia/lithium nitrate and ammonia/sodium thiocyanate. They concluded that ammonia/lithium nitrate obtained lower mass absorption transfer and absorber thermal load values than did the ammonia/water and ammonia/sodium thiocyanate in the three cases studied. This was mainly because its higher viscosity caused problems with the absorption of ammonia vapor in the ammonia/lithium nitrate solution.

As far as the present authors are aware, there have been no experimental studies regarding the absorption of ammonia vapor when using an ammonia/lithium nitrate solution or ammonia/(lithium nitrate + water) in a plate heat exchanger. The present paper presents the results of an experimental study aimed at evaluating the heat and mass transfer coefficients of this absorber configuration.

2. Description of the test facility

The experimental test facility was designed and built in order to study the absorption process in the channel of a plate heat exchanger in such a way that the operating parameters of interest could be adjusted. These parameters are: the solution and cooling water flow rates and temperatures, the ammonia concentration in the solution and the operating pressure in the absorber.

The absorber used in the experimental set-up is a corrugated plate heat exchanger provided by Alfa Laval with Chevron-L type corrugation (30 degrees from the plate vertical axis). The area of the heat exchanger is 0.1 m^2. The main geometrical characteristics of the plate are given in Fig. 1. The heat exchanger was formed by four plates, thus making three channels. The upflow of solution in the central channel is cooled by the downflow of water in the two external channels.

The test facility consists of three circuits: the solution circuit, the cooling water circuit, and the heating water circuit, as shown in Fig. 2.

The solution circuit is where the absorption process takes place in the test section. It consists of the absorber (ABS), two stainless steel tanks (ST and AT), a magnetic coupling gear pump, a heat exchanger (ICS), and a vapor–liquid separator (VLS).

Poor solution from the storage tank (ST) is pumped through the solution heat exchanger (ICS) to the bottom side of the absorber (ABS). In the ICS the solution is heated to the desired inlet temperature. In the channel of the plate heat exchanger, the upstream solution absorbs ammonia vapor fed from an ammonia bottle. Heat released by the absorption process is removed by the cooling water circuit. The rich solution leaves the absorber at the top and flows to the VLS, where the unabsorbed vapor is separated from the liquid phase and stored in tank AT. Finally, the solution is sent to storage tank ST.

Solution mixture and ammonia vapor flowed in co-current in the central channel, and cooling water flowed in countercurrent on both sides of the channel. Ammonia vapor was injected in bubble mode from an ammonia bottle using a thin tube with an internal diameter of 1.7 mm, as shown in Fig. 2.

The cooling water circuit consists of a 5-kW heater (R2), a magnetic flow meter (F), a pump, and a heat exchanger (HX1). The heating water circuit allows the solution to be preheated to a set temperature before entering the absorber. This circuit consists of a 5 kW heater (R1), a pump, a flow meter, and a heat exchanger (ICS).

RTD temperature sensors (T) and pressure transmitters (P) were used to register the temperature and pressure in the points shown in Fig. 2. Coriolis flow meters (C) were used to measure the density and flow rate of the poor and rich solutions. The solution concentration at the absorber inlet and outlet was determined from the density and temperature values measured by the Coriolis flow meter using the density correlation presented by Libotean et al. [18]. The Coriolis flow meter located at the absorber outlet was also used to determine the maximum amount of ammonia that can be absorbed

under certain conditions. When ammonia vapor is present at the absorber outlet, the density value measured by the Coriolis flow meter decreases significantly and becomes very unstable.

The thermodynamic and transport properties of the binary and ternary mixtures were calculated using the correlations presented by Libotean et al. [17,18]. Thermal conductivity of the binary mixture was calculated from the correlation reported by Cuenca et al. [19].

3. Data reduction

The design of the test bench makes it possible to perform experiments in which the following operating parameters are varied: solution mass flow, solution inlet temperature, cooling-water inlet temperature, solution inlet concentration, and system pressure. In each experiment, once the steady-state regime was reached, all operating conditions were recorded and maintained for about 25 minutes. The following sub-paragraphs summarize the methods used to calculate the absorber efficiency parameters.

3.1 NH_3 mass absorption flux

This parameter makes it possible to configure the system's capacity to absorb ammonia vapor from the evaporator. The NH_3 mass absorption flux (F_{AB}) is the absorbed mass flow rate of ammonia vapor per unit of heat transfer area, and it is expressed by the following equation:

$$F_{AB} = \frac{\dot{m}_{NH3,Absorbed}}{A_{exchange}} \tag{1}$$

3.2 Solution heat transfer coefficient

The test facility provides values of the overall heat transfer coefficient that depends on the heat transfer coefficient in the cooling water side, the solution heat transfer coefficient, and the plate wall heat transfer resistance. Since both coefficients are unknown, previous work was carried out to obtain the water side heat transfer coefficient. This coefficient (h_{Cw}) was determined experimentally by means of separate water-to-water experiments in the same test facility, using a modified Dittus-Boelter

equation combined with a least-square method. The data reduction procedure is described in the following sections.

The absorber thermal load is determined from the data measured on the water side.

$$Q = \dot{m}_{Cw} \cdot Cp_{Cw} \cdot (T_{Cw,Out} - T_{Cw,In}) \tag{2}$$

The overall heat transfer coefficient U is given by:

$$U = \frac{Q}{A \cdot LMTD} \tag{3}$$

where *LMTD* is the logarithmic mean temperature difference based on the measured solution and cooling-water temperatures at the absorber inlet and outlet. This *LMTD* definition was used because the *LMTD* based on saturation temperatures represents the idealized driving temperature difference for heat transfer in the absorption process, which is suitable when the solution temperature in the absorber is close to its saturation state. However, it was observed in the experiments that the bulk solution was subcooled trough the absorber.

$$LMTD = \frac{\left(T_{S,In} - T_{Cw,Out}\right) - \left(T_{S,Out} - T_{Cw,In}\right)}{\ln\left(\frac{T_{S,In} - T_{Cw,Out}}{T_{S,Out} - T_{Cw,In}}\right)} \tag{4}$$

The solution heat transfer coefficient is expressed by the following equation.

$$\frac{1}{h_S} = \frac{1}{U} - \left(\frac{1}{h_{Cw}} + \frac{e_W}{k_{Steel,W}}\right) \tag{5}$$

The water-side heat transfer coefficient (h_{cw}) was determined by carrying out preliminary experiments using water as the working fluid on both the cold and hot sides. The experimental data were correlated using Equations (6) and (7):

Transition regime (Re: 170-400):

$$Nu = 0.844 \cdot Re^{0.500} \cdot Pr^{1/3} \cdot \left(\frac{\mu}{\mu_W}\right)^{0.14} \tag{6}$$

Turbulent regime (Re: 400-1710):

$$Nu = 0.461 \cdot Re^{0.613} \cdot Pr^{1/3} \cdot \left(\frac{\mu}{\mu_W} \right)^{0.14} \quad (7)$$

In all the experimental results presented in this paper, the water-side heat transfer coefficient was between 25 and 200 % higher than the solution-side heat transfer coefficient. By keeping the coolant heat transfer coefficient high, the solution side resistance becomes dominant and the effect of the coolant-side heat transfer coefficient is minimized, which in turn yields low uncertainties in the absorption heat transfer coefficients.

3.3 Degree of sub-cooling of the solution leaving the absorber

The degree of sub-cooling of the solution leaving the absorber (ΔT_{sub}) represents the degree to which the available absorption potential is used, and it is equal to the difference between the actual outlet solution temperature and the equilibrium solution temperature at the absorber pressure and the actual outlet solution concentration:

$$\Delta T_{Sub} = \left(T_{S,Eq,Out} - T_{S,Out} \right) \quad (8)$$

3.4 Mass transfer coefficient

The mass transfer coefficient was calculated by applying the same concept as for the overall heat transfer coefficient and is expressed as follows:

$$K_m = \frac{\dot{m}_{NH3,Absorbed}}{A \Delta X_{lm}} \quad (9)$$

The logarithmic mean concentration difference, ΔX_{lm}, expresses the nominal log-mean concentration difference along the absorber channel

$$\Delta X_{lm} = \frac{\left(X_{Sat,S} \rho_{Sat,S} - X_S \rho_S \right)_{In} - \left(X_{Sat,S} \rho_{Sat,S} - X_S \rho_S \right)_{Out}}{\ln \frac{\left(X_{Sat,S} \rho_{Sat,S} - X_S \rho_S \right)_{In}}{\left(X_{Sat,S} \rho_{Sat,S} - X_S \rho_S \right)_{Out}}} \quad (10)$$

The saturation concentrations in Eq. (10) were determined on the basis of the measured temperatures and pressures using the correlations reported by Libotean et al. [17].

3.5 Uncertainty analysis

The measurement system recorded temperatures, pressures, mass flow rate and density of solution and volumetric flow rate and temperatures of coolant. The uncertainties of all the calculated parameters were analyzed by the procedure described in NIST Technical Note 1297 (Taylor and Kuyatt [23]) and implanted in the EES software. Table 1 summarizes the error considered in the measured variables and the maximum uncertainty (95% CL) obtained in the absorber parameters.

4. Results and discussion

The most significant experimental results obtained in the absorber test bench with the binary ammonia/lithium nitrate and ternary ammonia/(lithium nitrate + water) fluid mixtures are presented below. The operating conditions considered for temperature, pressure, solution mass flow, and concentrations (Table 2.) were determined from numerical simulations of the single-effect absorption refrigeration cycle at evaporation and condensation/absorption temperatures of 5 ºC and 40 ºC, respectively. In the experiments performed with the ternary mixture, the water content in the absorbent (water + lithium nitrate) was set to a constant value of 25 % by weight, given that rectification is not required for the absorption cycle under these conditions [17].

4.1 Absorber operating with ammonia/lithium nitrate

This section presents the results of a sensitivity study performed to analyze how the solution mass flow rate, cooling-water temperature and mass flow rate and ammonia concentration of the ammonia/lithium nitrate mixture affect the absorber performance parameters.

4.1.1 Effect of the solution mass flow rate and cooling-water operating conditions

Fig. 3(a-d) shows the ammonia mass absorption flux, the solution heat transfer coefficient, the subcooling and the mass transfer coefficient as a function of the solution Reynolds number and cooling-water inlet temperature, respectively. The effect of the water-side flow rate on the solution heat tranfer coefficient is also discussed.

The mass absorption flux (Fig. 3a) increases almost linearly from 0.0029 to 0.0062 kg/m^{2}s when the solution Reynolds number increases from 15 (solution mass flow rate of 15.8 kg/h) to 49 (51 kg/h) at 35 ºC of cooling-water temperature entering the absorber. However, when the cooling-water inlet temperature is set to 40 ºC, the mass absorption flux increases from 0.0017 to a maximum of 0.0043 kg/m^{2}s, thus giving a solution Reynolds number of 45, after which it remains almost constant. The improvement in the mass absorption flux as the cooling-water inlet temperature decreases is due to the fact that a lower cooling-water temperature implies a higher temperature difference between the solution and cooling water streams. This increases the capacity of the absorber to dissipate the heat released by the absorption process, which in turn significantly improves the absorption potential of the heat exchanger.

Fig. 3b shows that the solution heat transfer coefficient also increases almost linearly from 1.8 to 4.0 kW/m^{2}K and from 2.0 to 5.5 kW/m^{2}K at cooling-water temperatures of 35 ºC and 40 °C at the absorber inlet, respectively. For the solution-side heat transfer coefficient the trend is reversed, resulting in a lower heat transfer coefficient as the cooling-water temperature decreases. A lower cooling-water temperature at the absorber entrance causes a higher absorber thermal load and a higher logarithmic mean temperature difference. However, the increase in the LMTD is higher than that of the absorber thermal load, which causes the heat transfer coefficient to drop. This trend of the solution heat transfer coefficient as the cooling-water temperature decreases is not observed when the LMTD definition based on saturation temperatures is used.

Fig. 3c shows the effect of the solution Reynolds number on subcooling when the inlet cooling water temperature is varied. As can be seen in Fig. 3c the subcooling increases when the solution Reynolds number increases. The subcooling is similar for both inlet water temperatures and ranges between 4 and 6 °C.

The effect of the solution Reynolds number on the mass transfer coefficient is illustrated in Fig. 3d. These results indicate that the mass transfer coefficient increases with solution Reynolds number and decreases with the cooling water temperature.

The experiments of the 3 points in colour in Fig. 3 were performed at a cooling-water temperature of 40 °C, a solution Reynolds number around 50 and a mass flow rate of cooling-water of 333 (red), 198 (green) and 174 kg/h (blue). The correponding solution-side heat transfer coefficients are 6.8, 7.4 and 10.0 kW/m^{2}K, respectively. This heat transfer coefficient becomes smaller when the cooling water flow rate increases because

the increase in absorber thermal load is lower than the increase in the LMTD. Fig. 3b shows that the reduction in the solution heat transfer coefficient is about 50 %. This increase in cooling water flow rate results in a more modest mass absorption flux improvement of 22 %, as can be seen in Fig. 3a.

As the water-side flow rate increases, the solution outlet temperature decreases and causes the increase in subcooling. Although the mass absorption flux increases, the outlet temperature decreases at a faster rate thereby increasing the subcooling. Also, these 3 points indicate that as the water-side flow rate increases, the mass transfer coefficient increases. This is attributed to the fact that an increase in cooling water flow rate causes a decrease in solution temperature that, as indicated by the results in Fig. 3d, improves the mass transfer coefficient.

4.1.2 Effect of the solution ammonia concentration

Fig. 4a and 4b show the mass absorption flux and solution heat transfer coefficient as a function of the solution Reynolds number at ammonia mass fractions of 0.450, 0.465 and 0.480 in the solution entering the absorber. The cooling-water and solution temperatures at the absorber entrance were 35 ºC and 45 ºC, respectively, and the cooling flow rate was kept between 130 and 170 l/h. The ammonia concentration reduces the solution viscosity. Thus, higher solution Reynolds numbers were achieved for the same solution mass flow rates.

When the inlet concentration of the solution increases, the saturation pressure of solution increases. It reduces the pressure difference between absorber and solution and consequently decreases the absorption capacity. This can be seen in Fig. 4a where the mass absorption flux increases slightly from 0.0024 to 0.0028 kg/m^{2}s when the solution Reynolds number increases from 25 to 69 at an ammonia mass fraction of 0.480 in the solution entering the absorber, whereas the corresponding interval increase is from 0.0029 to 0.0062 kg/m^{2}s when the solution Reynolds number increases from 11 to 50 and an ammonia mass fraction of 0.450 in the solution. For instance, when the ammonia mass fraction was increased from 0.450 to 0.480, at a solution Reynolds number of around 50, the absorption mass flux was reduced to a third part of the initial value. Moreover, a higher ammonia concentration in the solution implies that the solution Reynolds number has a less pronounced effect on the mass absorption flux.

The solution-side heat transfer coefficient increases from 1.3 to 2.4 kW/m^2 K when the solution Reynolds number is increased from 25 to 69 with an ammonia mass fraction of 0.480 in the solution entering the absorber. Moreover, the solution-side heat transfer coefficient increases from 1.5 to 4.0 kW/m^2 K when the solution Reynolds number is increased from 11 to 50 with an ammonia mass fraction of 0.450 in the solution. The improvement in the solution-side heat transfer coefficient as the solution Reynolds number increases is less pronounced at higher ammonia mass fractions in the solution entering the absorber.

Fig. 4c depicts the outlet solution subcooling with the solution Reynolds number for different inlet solution concentrations. The subcooling increases when the inlet solution concentration decreases and the solution Reynolds number increases. However, the increase ratio decreases with the inlet solution concentration. For the three concentrations studied (45, 46.5 and 48 %) the subcooling of the solution leaving the absorber ranges from 4.2 to 6.7 ºC, 4.6 to 5.5 ºC and 3.7 to 4.2 ºC, respectively.

Finally, Fig. 4d shows the mass transfer coefficient with varying solution Reynolds number for two inlet solution concentrations. This figure does not include the results corresponding to an inlet solution concentration of 48 % because this concentration is close to the saturation concentration and the error when calculating the mean concentration difference, ΔX_{lm}, is very high and may lead to a large dispersion of the result. As the Fig. 4d shows, the mass transfer coefficient increases with the solution Reynolds number and there are small differences between both concentrations. For the two concentrations presented (45 and 46.5) the mass transfer coefficient ranges from a minimum of 0.6 m/h to a maximum of 1.4 m/h. Note that for both concentrations, the increase in the rate of heat transfer coefficient is larger than that of the mass transfer coefficient.

4.2 Comparison of absorber performance with the ammonia/lithium nitrate binary mixture and the ammonia/(lithium nitrate + water) ternary mixture

The results achieved with ammonia/lithium nitrate and ammonia/(lithium nitrate + water) were compared at an absorber pressure of 510 kPa; an ammonia mass fraction of the solution entering the absorber of 0.450 and 0.435 for the binary and ternary mixtures, respectively; an absorbent water content of 25 % by weight for the ternary

mixture; and solution and cooling-water temperatures of 45 ºC and 40 ºC, respectively, at the absorber entrance. In order to establish a similar absorption potential for both fluid mixtures, the ammonia mass fraction of the ternary mixture was determined using the same concentration gradient from equilibrium at the absorber entrance as that which was used for the binary mixture.

Fig. 5a and 5b show that the lower viscosity of the ammonia/(lithium nitrate + water) ternary mixture and the introduction of a third component with a high affinity for ammonia enhance the heat and mass transfer processes taking place in the absorber. Under the operating conditions considered in this comparison, the viscosity of the binary fluid mixture entering the absorber is around 5.93 cP, whereas that of the ternary fluid mixture is about 2.84 cP. In Fig. 5, the parameters characterizing absorber efficiency are depicted using the solution flow rate instead of the solution Reynolds number because the lower viscosity of the ternary mixture leads to a higher Reynolds number.

The mass absorption flux achieved with the ternary mixture ranges from 0.004 to 0.00595 kg/m^{2}s, which is between 1.3 and 1.6 times higher than that obtained with the binary mixture under the same operating conditions, whereas the solution-side heat transfer coefficient for the ternary mixture ranges from 3.5 to 8.1 kW/m^{2}K, which is around 1.4 times higher than that of the binary mixture.

Fig. 5c depicts the subcooling of the solution leaving the absorber versus the solution flow rate for both fluid mixtures. The decrease in subcooling due to the addition of water to the absorbent is very significant. When the ternary mixture is used as the working fluid, the solution leaves the absorber very close to the equilibrium, with the maximum sub-cooling being around 2.3 °C at the higher solution flow rate.

When the mass absorption flux and heat transfer coefficient are compared against solution Reynolds number, the results obtained with both mixtures at the same Reynolds are very close. This can be seen in Fig. 6 where the mass absorption flux and heat transfer coefficient achieved with both mixtures are compared against solution Reynolds number.

5. Nusselt and Sherwood numbers correlations

Empirical correlations for the solution Nusselt and Sherwood numbers are proposed on the basis of the experimental data presented here for the absorption of ammonia vapor

by ammonia/lithium nitrate solution in a plate heat exchanger. The correlations were developed using only the experimental data of the binary mixture because the thermal conductivity of the ternary mixture is not available for calculating the Nusselt number and also due to the fact that there was a large scatter in the calculated values of the mass transfer coefficient for the ternary fluid mixture that leaves the absorber at almost equilibrium conditions (small values of subcooling).

On the basis of data presented for the binary mixture, the Nusselt and Sherwood numbers were correlated as follows:

$$Nu = 0{,}24 \cdot \mathrm{Re}^{0,8} \cdot \mathrm{Pr}^{1/3} \cdot \left(\frac{T_{eq,In}}{T_{S,In}} \right)^{6.6} \cdot \left(\frac{T_{S,In}}{T_{Cw,In}} \right)^{-0.9} \quad (11)$$

$$Sh = 800 \cdot \mathrm{Re}^{0.90} \cdot Sc^{0.17} \cdot \left(\frac{T_{eq,Ent}}{T_{S,In}} \right)^{-5.11} \cdot \left(\frac{T_{S,In}}{T_{Cw,In}} \right)^{-1} \quad (12)$$

Fig. 6(a) indicates that correlation (11) can satisfactorily predict 82.1 % of the experimental data of the solution heat transfer coefficient at a margin of error lower than 15 %. Similarly, correlation (12) can predict 90% of the mass transfer coefficient data at a margin of error of less than 15%. Moreover, these correlation equations can represent our data with average deviation of 9.4 % and 3.7 % for the heat transfer coefficient and mass transfer coefficient, respectively. The values of the fit parameter, R2, of correlations (11) and (12) are indicated in Figure (7)

6. Conclusions

This paper presents the results of experiments on the absorption process in a plate heat exchanger of ammonia in a binary mixture of ammonia/lithium nitrate and a ternary mixture of ammonia/(lithium nitrate + water) with an absorbent water content of 25 %, under operating conditions of interest for absorption chillers. The following conclusions can be drawn from this study:

- For both the binary and ternary mixtures, the mass absorption flux, heat transfer coefficient, subcooling and mass transfer coefficient increase as the solution flow rate increases.
- The mass absorption flux achieved with the binary mixture is enhanced around 1.38 and 1.73 times as the cooling-water inlet temperature decreases because the concentration gradient between the actual solution leaving the absorber and

equilibrium state is increasing. This trend is reversed for the solution-side heat transfer coefficient which decreases around 0.69 and 0.87 times. This is attributed to a limiting heat transfer process in the absorber at lower cooling-water inlet temperatures. Moreover, increasing the concentration of ammonia in the binary mixture by 3 % by weight significantly reduces the capacity of the mixture to absorb ammonia due to the approach to the saturation concentration at the operating conditions under study. When the ammonia mass fraction was increased from 0.450 to 0.480, at a solution Reynolds number of around 50, the absorption mass flux was reduced to a third part of the initial value.

- The ternary mixture's lower viscosity and the high affinity of ammonia for water mean that the heat and mass transfer processes taking place in the absorber are significantly better for this mixture than for the binary mixture. The mass absorption flux and the solution heat transfer coefficient achieved with the ternary mixture are around 1.3-1.6 and 1.4 times higher, respectively, than those of the binary mixture under similar operating conditions.
- The present study has provided empirical correlations for the Nusselt and Sherwood numbers of mass and heat transfer governing the absorption of ammonia by the ammonia/lithium nitrate solution in a PHE. Both correlations can satisfactorily predict around 80 to 90 % of the experimental data of the solution heat and mass transfer coefficients at a margin of error lower than 15 %.

Acknowledgements

The authors would like to acknowledge the funding for this work provided the Spanish Ministries of Education and Science (ENE2005-03346) and Science and Innovation (ENE2008-00863). Carlos Amaris acknowledges the Spanish Ministry of Science and Innovation for the award of a scholarship (BES-2009-015241).

References

[1] R. Salgado, A. Burguete, M.C. Rodríguez, P. Rodríguez, Simulation of an absorption based solar cooling facility using a geothermal sink for heat rejection,

Proceedings of The First International Conference on Solar Heating, Cooling and Buildings, EUROSUN, Lisbon, Portugal, 2008, October 7-10.

[2] K. Gensch, Lithiumnitratammoniakat als Absorptionsflüssigkeit für Kältemaschinen, Zeitschrift für die gesamte Kälte, Industrie, 1937, Heft 2, S. 24 – 30.

[3] K.A. Antonopoulos, E.D. Rogdakis, Performance of solar driven ammonia-lithium nitrate and ammonia-sodium thicyanate absorption systems operating as coolers or heat pumps in Athens, Applied Thermal Engineering (16) (1996) 127-147.

[4] D-W Sun, Comparison of the performances of NH_3-H_2O, NH_3-$LiNO_3$ and NH_3-NaSCN absorption refrigeration systems, Energy Conversion Management (39) (1998) 357-368.

[5] C.A. Infante Ferreira, Operating characteristics of NH_3-$LiNO_3$ and NH_3-NaSCN absorption refrigeration machines, Proceedings of The Nineteenth International Congress of Refrigeration, Vol. IIIa, 1995, 321-328.

[6] J.M. Abdulateef, K. Sopian, M.A. Alghoul, Optimum design for solar absorption refrigeration systems and comparison of the performances using ammonia-water, ammonia-lithium nitrate and ammonia-sodium thiocyanate solutions. International Journal of Mechanical and Materials Engineering, 3 (1) (2008) 17-24.

[7] R. Ayala, J.L. Frías, C.L. Heard, F.A. Holland, Experimental assessment of and ammonia/lithium nitrate absorption cooler operated on low temperature geothermal energy, Heat Recovery Systems & CHP, 14 (1994) 437-446.

[8] C.L. Heard, R. Ayala, R. Best, An experimental comparison of an absorption refrigerator using ammonia/water and ammonia/lithium nitrate, Proceedings of The Ab-Sorption 96, Montreal, Canada, 1996, Vol.1, pp 245-252.

[9] H.J. Ehmke, M. Renz, Ternary working fluids for absorption systems with salt-liquid mixtures as absorber, IIF - IIR Congress, Commission B1. Paris, France, 1983, August. 31-September 7.

[10] H. Bokelmann, Presentation of new working fluids for absorption heat pumps, Absorption Heat Pump Congress. Paris, France, 1985, March 20 – 22.

[11] R.H. Reiner, A. Zaltash, Evaluation of ternary ammonia/water fluids for GAX and regenerative absorption cycles. Report ORNL/CF-91/263,1991.

[12] H.L. Ehmke, Stoffsysteme für absorptionswarmepumpen-experimentelle bestimmung thermophysikalischer eigenschaften von lösungen der kältemittel methylamin, ammoniak und monochlordifluormethan (R22), PhD thesis, Universität Essen, Essen, Germany, 1984.

[13] A. Manago, Research and development on working fluids, working fluids and transport phenomena in advanced absorption heat pumps, ANNEX 14, Final report, 1995, Vol. 2, 4-1.

[14] R.H Reiner, A. Zaltash, Densities and Viscosities of ternary Ammonia/Water Fluids, ASMe Winter Annual Meeting, New Orleans, 1993, November 28-December 3.

[15] A. Bothe, Das Stoffsystem NH_3-$LiNO_3$/H_2O für den Einsatz in Absorptionkreisläufen. PhD thesis, Universität Essen, Essen, Germany, 1989.

[16] G. Moreno-Quintanar, W. Rivera, R. Best, Comparison of the experimental evaluation of a solar intermittent refrigeration system for ice production operating with the mixtures NH_3/$LiNO_3$ and NH_3/$LiNO_3$/H_2O. Renewable energy (38) (2012) 62-68.

[17] S. Libotean, D. Salavera, M. Valles, X. Esteve, A. Coronas, Vapour-Liquid Equilibrium of Ammonia+Lithium Nitrate+Water and Ammonia+Lithium Nitrate Solutions from (293.15 to 353.15) K; J. Chem. Eng. Data 52 (2007) 1050-1055.

[18] S. Libotean, A. Martin, D. Salavera, M. Valles, X. Esteve, A. Coronas, Densities, Viscosities, and Heat Capacities of Ammonia + Lithium Nitrate and Ammonia + Lithium Nitrate + Water Solutions between (293.15 and 353.15) K, J. Chem. Eng. Data 53 (10) (2008), 2383–2388.

[19] Y. Cuenca, M. Vallès, A. Vernet, Thermal conductivity of ammonia-lithium nitrate, International Sorption Heat Pump Conference. Padua, Italy, 2011, April 6-8.

[20] Eysseltová, Orlova, IUPAC-NIST Solubility Data Series. 89. Alkali Metal Nitrates. Part 1. Lithium Nitrate. Journal of Physical and Chemical Reference Data 39 (2010), art. no. 033104.

[21] C.A. Infante Ferreira, Vertical Tubular Absorbers for Ammonia-salt Absorption Refrigeration, PhD thesis, Delft Technical University, Delft, Holland, 1985.

[22] J. Cerezo, R. Best, R.J. Romero, A study of a bubble absorber using a plate heat exchanger with NH_3-H_2O, NH_3-$LiNO_3$ and NH_3-NaSCN, Applied Thermal Engineering 31 (2011) 1869-1876.

[23] B.N. Taylor, C.E. Kuyatt, Guidelines for Evaluating and Expressing the Uncertainty of NIST Measurement Results, National Institute of Standards and Technology Technical Note 1297, 1994.

Table

Table 1. Summary of the uncertainty analysis

Parameters	Uncertainty
PHE geometry	
Width, thickness and pitch, L (%)	± 0.5
Area of plate, A (%)	± 0.5
Sensors	
Temperature, T (ºC)	± 0.1
System pressure, P (%)	± 0.25
Solution mass flow rate, $\dot{m}_S$ (%)	± 0.1
Solution density, ρ_S (kg/m^3)	± 0.5
Coolant flow rate, V_{CW} (l/h)	± 0.24
Calculated parameters	
Solution Reynolds number, Re (%)	6.0
Absorption mass flux, F_{AB} (%)	5.8
Solution heat transfer coefficient, h_S (%)	21.4
Solution mass transfer coefficient, Km (%)	18.8

Table 2. Operating conditions

Parameters	**Range**
Solution temperature at the absorber inlet, °C	45
Cooling-water temperature at the absorber inlet, °C	35.0-40.0
Ammonia mass fraction of the solution at the absorber inlet (binary mixture)	0.45-0.48
Ammonia mass fraction of the solution at the absorber inlet (ternary mixture)	0.435
Water content in the absorbent of the ternary mixture	0.25
Absorber pressure, kPa	510
Solution mass flow rate, kg/h	15.0-60.0
Cooling water flow rate, kg/h	130-333
Vapour mass flow rate, kg/h	0.6-2.2

Figure

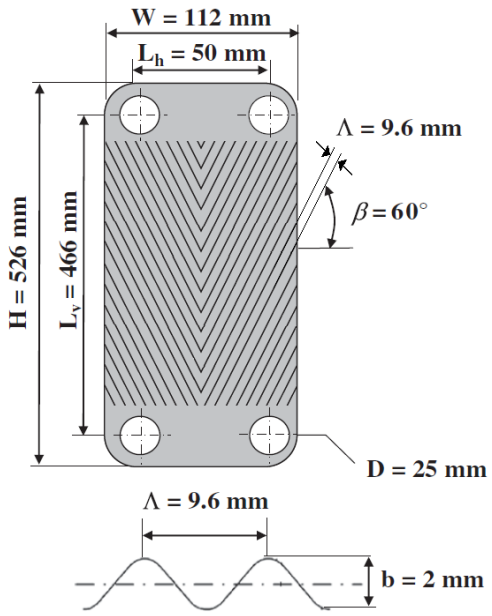

Figure 1. Geometrical characteristics of the plate heat exchanger

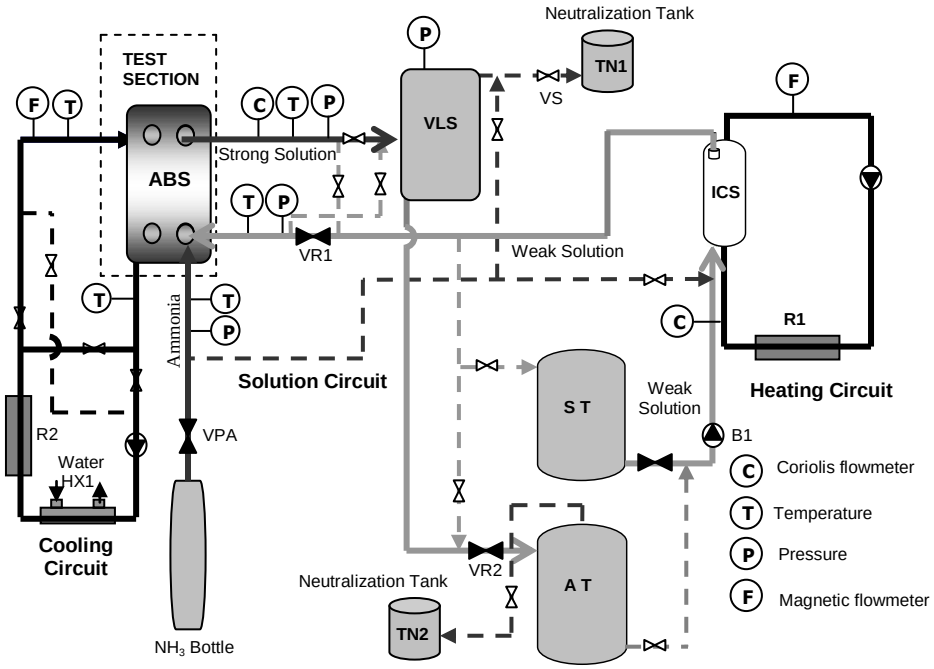

Figure 2. Outline of the absorber test facility

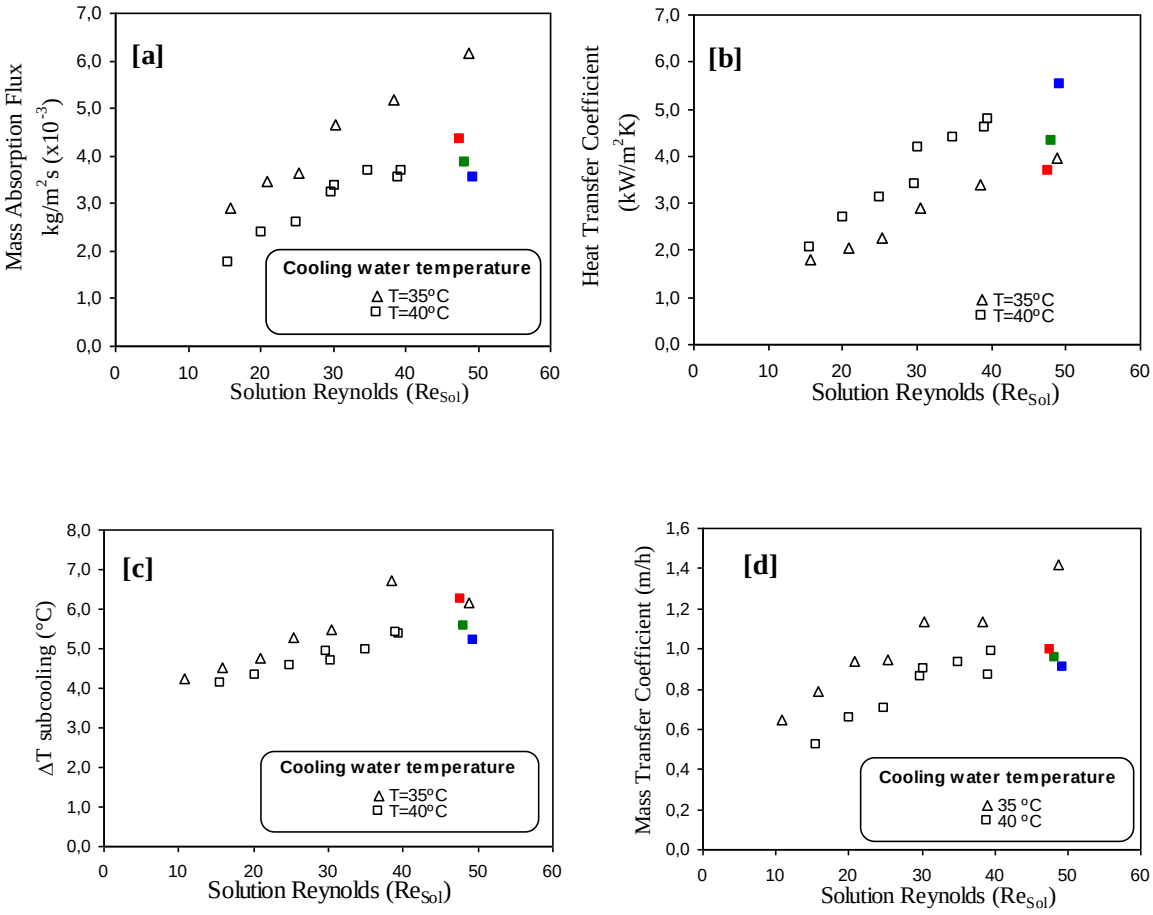

Figure 3. Effect of the solution Reynolds number and cooling-water temperature on: (a) mass absorption flux, (b) solution heat transfer coefficient, (c) subcooling and (d) mass transfer coefficient

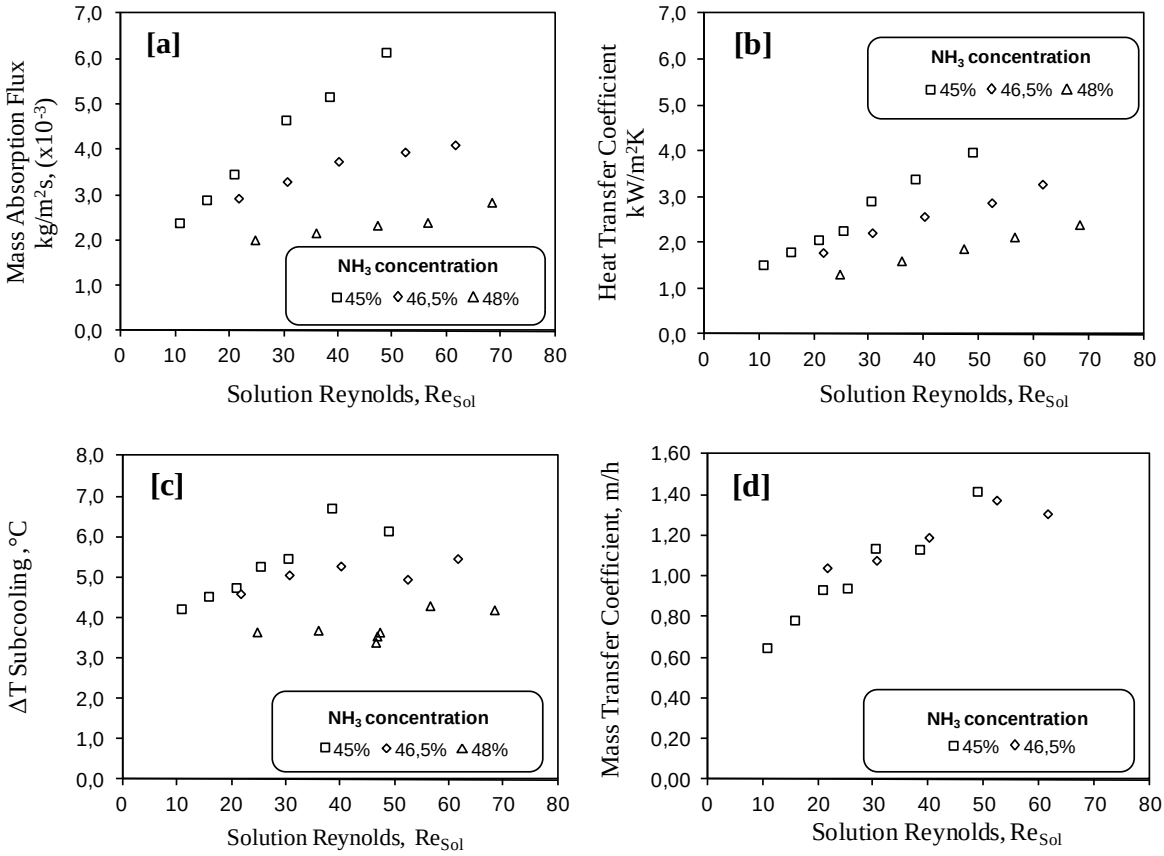

Figure 4. Effect of NH_3 concentration on: (a) mass absorption flux, (b) solution heat transfer coefficient, (c) subcooling and (d) mass transfer coefficient

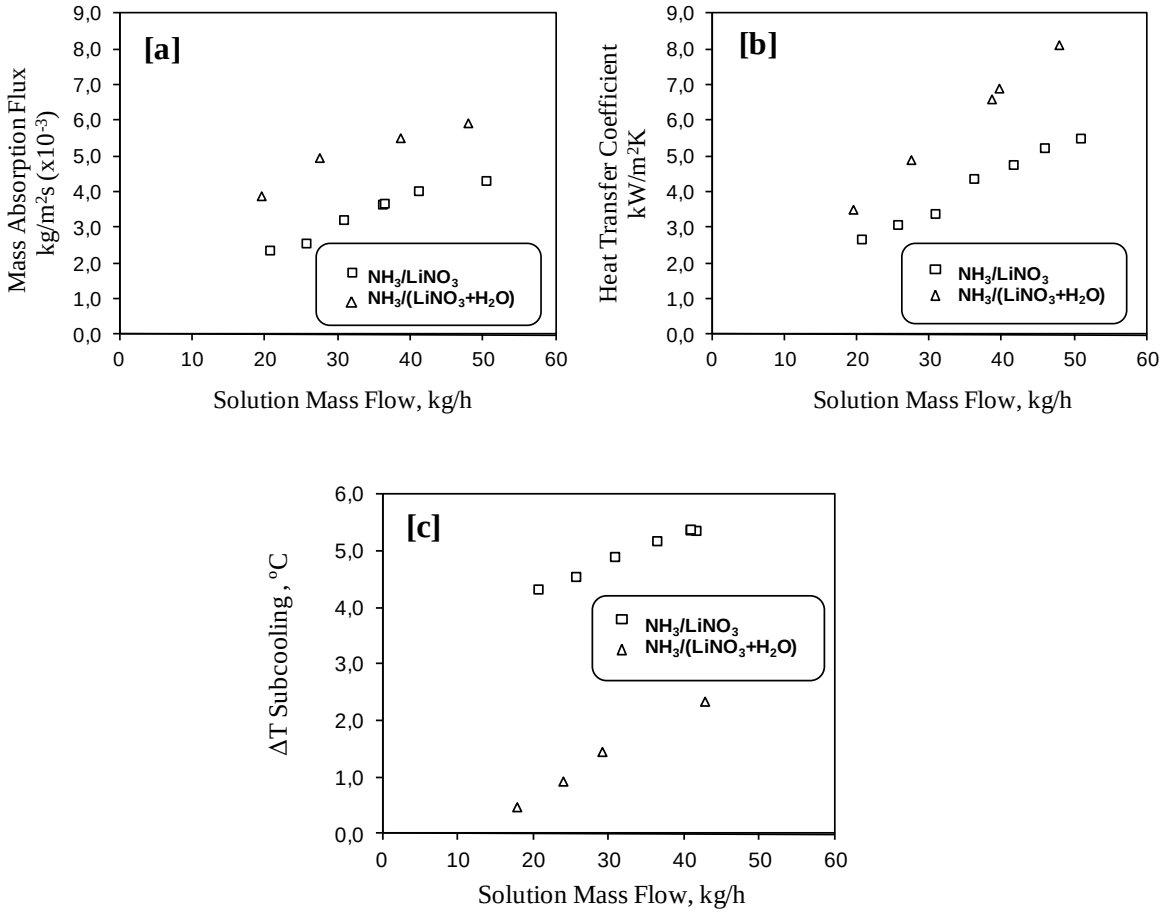

Figure 5. Effect of the solution mass flow on: (a) mass absorption flux and (b) solution heat transfer coefficient and (d) subcooling for $NH_3/LiNO_3$ and $NH_3/(LiNO_3+H_2O)$ mixtures

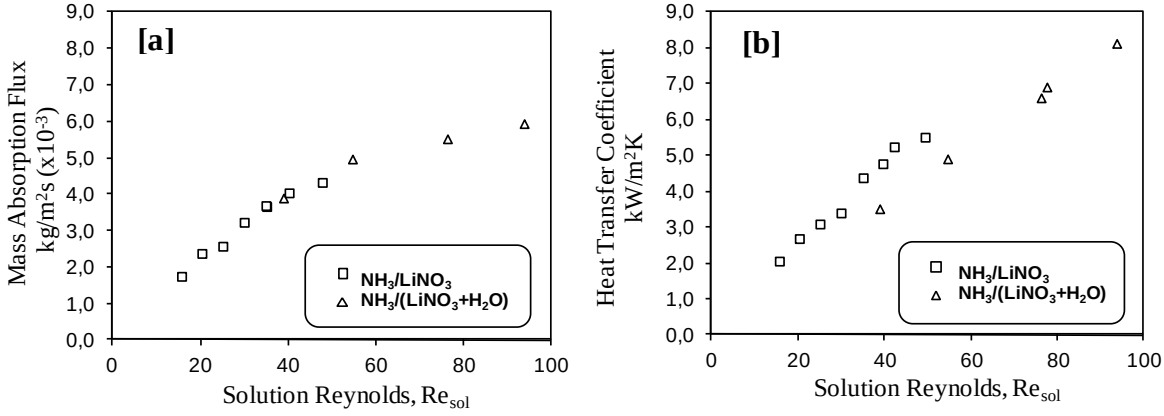

Figure 6. Effect of the solution Reynolds number on: (a) mass absorption flux and (b) solution heat transfer coefficient for $NH_3/LiNO_3$ and $NH_3/(LiNO_3+H_2O)$ mixtures

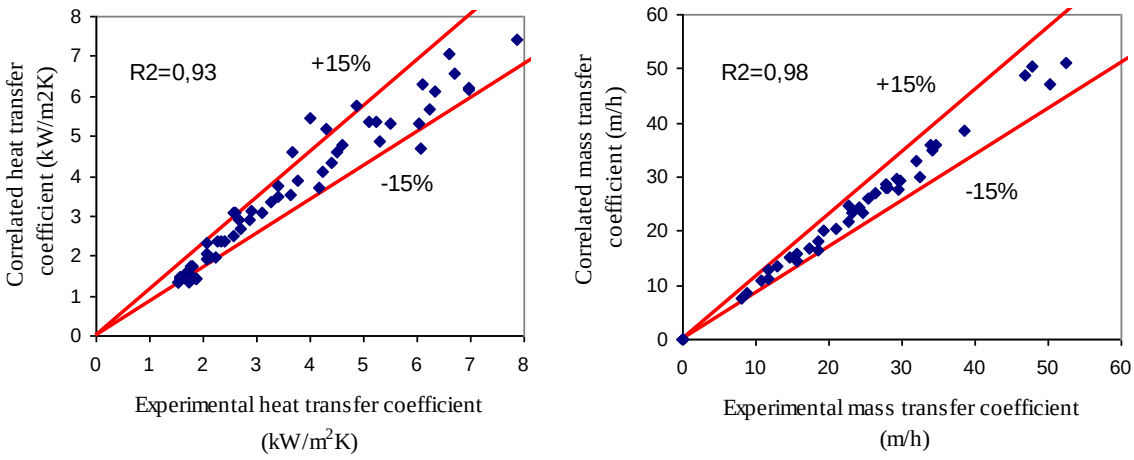

Figure 7. Comparison of the correlations' predictions with experimental data for: (a) heat transfer coefficient; (b) mass transfer coefficient